the terra material contains a large amount of the mineral anorthite, which has low density and a high melting point. Similar ideas based on the preliminary results of this alpha-scattering experiment have recently been presented by Anderson *et al.* and Wood *et al.* (*14*).

As indicated above, the differentiation process that produced this crust on the moon had some similarities to, but in general was different from, the process that occurred on earth. A particular difference was in the apparent behavior of uranium and thorium. On the earth, the granitic crust is enriched in these elements relative to the basalts. The Surveyor data on the alpha radioactivity of the lunar surface (*21*) indicate a lower uranium content at the terra site of Surveyor 7 than at Mare Tranquillitatis. The data of Luna 10 (*22*) also gave some indication of a lower content of radioactive elements in the terrae than in the maria. Thus, there is no evidence for an enrichment of uranium in the terrae of the moon. On the moon, in the absence of an oxidizing medium and water, it may be that both uranium and thorium followed the chemistry of +4 elements and stayed with elements such as titanium and zirconium. The rather high concentration of these elements, which appears to be a characteristic of mare material, may mean that on the moon, in contrast to the assumed situation on earth, the heat production due to the radioactive decay of the heaviest elements has been buried below the crust. At early times this factor could have been an important one in the history of the moon.

JAMES H. PATTERSON
*Chemistry Division, Argonne National Laboratory, Argonne, Illinois 60439*
ANTHONY L. TURKEVICH*
*Enrico Fermi Institute* and *Department of Chemistry, University of Chicago, Chicago, Illinois 60637*
ERNEST J. FRANZGROTE
*Jet Propulsion Laboratory, Pasadena, California 91103*
THANASIS E. ECONOMOU
KENNETH P. SOWINSKI
*Enrico Fermi Institute, University of Chicago*

### References and Notes

1. A. L. Turkevich, E. J. Franzgrote, J. H. Patterson, *Science* **158**, 635 (1967).
2. ———, *ibid.* **165**, 277 (1969).
3. A. L. Turkevich, J. H. Patterson, E. J. Franzgrote, *ibid.* **160**, 1108 (1968).
4. E. J. Franzgrote, J. H. Patterson, A. L. Turkevich, T. E. Economou, K. P. Sowinski, *ibid.* **167**, 376 (1970).
5. Lunar Sample Preliminary Examination Team, *ibid.* **165**, 1211 (1969).
6. E. M. Shoemaker, R. M. Batson, H. E. Holt, E. C. Morris, J. J. Rennilson, E. M. Walker, *J. Geophys. Res.* **74**, 6081 (1969).
7. A. L. Turkevich, E. J. Franzgrote, J. H. Patterson, *Science* **162**, 117 (1968).
8. J. H. Patterson *et al.*, *J. Geophys. Res.* **74**, 6120 (1969).
9. J. H. Patterson, A. L. Turkevich, E. J. Franzgrote, *ibid.* **70**, 1311 (1965); A. L. Turkevich, K. Knolle, E. J. Franzgrote, J. H. Patterson, *ibid.* **72**, 831 (1967).
10. R. F. Scott and F. I. Roberson, *ibid.* **74**, 6175 (1969).
11. R. A. Phinney *et al.*, *ibid.*, p. 6053.
12. R. R. Keays, R. Ganapathy, J. C. Laul, E. Anders, G. F. Herzog, P. M. Jeffery, *Science* **167**, 490 (1970).
13. A. L. Turkevich, J. H. Patterson, E. J. Franzgrote. *Amer. Sci.* **56**, 312 (1968).
14. A. T. Anderson, Jr. *et al.*, *Science* **167**, 587 (1970); J. A. Wood, J. S. Dickey, Jr., U. B. Marvin, B. N. Powell, *ibid.*, p. 602.
15. J. Green and A. Poldervaart, *Geochim. Cosmochim. Acta* **7**, 177 (1955).
16. K. C. Condie, *Science* **155**, 1013 (1967).
17. J. A. O'Keefe, *ibid.* **162**, 1405 (1968).
18. S. K. Runcorn and M. H. Shrubsall, *Phys. Earth Planet. Interiors* **1**, 317 (1969).
19. W. M. Kaula, *Science* **166**, 1581 (1969).
20. F. R. Boyd, *ibid.* **145**, 13 (1964); G. W. Wetherill, *ibid.* **160**, 1256 (1968).
21. A. L. Turkevich, J. H. Patterson, E. J. Franzgrote, K. P. Sowinski, T. E. Economou, *ibid.* **167**, 1722 (1970).
22. A. P. Vinogradov, Yu. A. Surkov, G. M. Chernov, F. F. Kirnozov, G. B. Nazarkina, *Geochimiya* **8**, 891 (1966).
23. The work at the Argonne National Laboratory was under the auspices of the U.S. Atomic Energy Commission. At the University of Chicago, the work was aided by NASA grant NGR-14-001-128; at the Jet Propulsion Laboratory by NASA contract NAS-7-100. We thank Professors N. Sugarman, E. Anders, and R. Clayton of the University of Chicago for critical help in the preparation of this report.
* Temporary address: Chemistry Department, Yale University, New Haven, Conn. 06520.

30 January 1970

## Phobos: Preliminary Results from Mariner 7

*Abstract*. *Analysis of an image of Phobos on Mariner 7 frame 7F91 indicates that the martian satellite is larger and has a darker surface than had previously been thought. The limb profile measures 18 by 22 kilometers and is elongated along the orbital plane. Phobos has an average visual geometric albedo of 0.065 lower than that known for any other body in the solar system. It seems probable that Phobos did not form by accretion around primordial Mars, but was captured at some later time.*

An objective of the Mariner 69 television experiment (*1*) was to photograph one or both of the two martian satellites, Phobos and Deimos, under conditions which would lead to estimates of their physical size and reflectivity. Throughout the far-encounter sequences of photographs taken by Mariners 6 and 7, Phobos and Deimos moved in and out of the field of view,

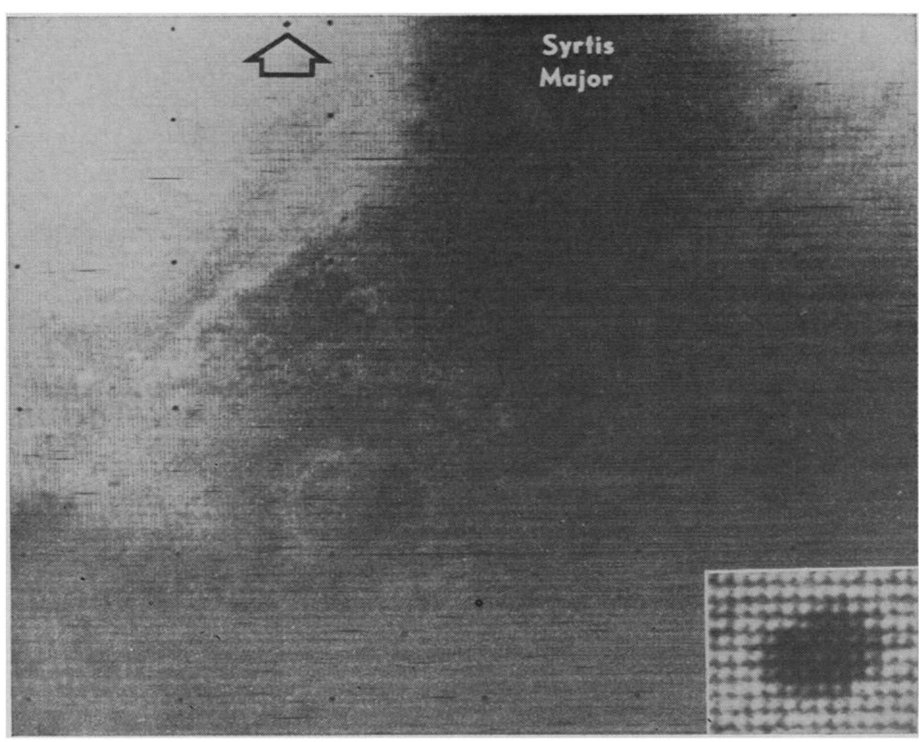


Fig. 1. Phobos as recorded on Mariner frame 7F91, with a $\times$ 15 enlargement (insert). A part of Syrtis Major is seen near the top. The phase angle is 22° and the range is 130,900 km to Phobos and 137,000 km to the martian surface.

alternately passing across and behind the disk of Mars. In addition to this random coverage, far-encounter frames 6F40 and 6F41 were timed so that both Phobos and its penumbral shadow on the martian surface could be simultaneously recorded (*2*). We have positive identification of the image of Phobos seen against the disk of Mars on three frames (7F69, 7F79, and 7F91) and tentative identification on three others (6F39, 7F53, and 7F66). We have been unable to identify either Phobos or its shadow on 6F40/41, and no convincing images of Deimos have been located. However, it is important to emphasize that computer processing of the Mariner 69 far-encounter pictures is still in a preliminary state, and that additional data regarding the satellites may emerge as processing techniques improve.

Only on frame 7F91 is the projected area of Phobos greater than a few pixels (picture elements), and I report here the results of preliminary measurements derived from the raw data of this frame. First-order noise removal, geometric correction, and photometric decalibration have been applied by hand, pixel by pixel, to the immediate part of 7F91 that includes and surrounds the image of Phobos (Fig. 1).

From smoothed photometric profiles of scan lines and pixel columns across the image of Phobos, I obtained a series of isophotometric contours that define the dark image of Phobos against a semibright region in Aeria just west of Syrtis Major. As seen by the spacecraft at a phase angle of 22°, the surface brightness of this part of Mars was approximately 1315 mlam. The actual isophotometric contour corresponding to the geometric edge of Phobos cannot be precisely determined because knowledge of the combined electronic-optical, point-spread function of the Mariner television system is limited. However, quite independently of our knowledge of image smear, it is possible to assess accurately the total light removed from the uniformly bright surface on which the soft-edged image of Phobos is seen. This is found to be 27,000 mlam-pixels and represents the product of the area of the geometric projection of Phobos and the difference between the martian surface brightness and the mean surface brightness of Phobos. This relation in turn defines the reflectivity of Phobos in terms of its physical size (*3*).

Two methods were used to evaluate the specific isophotometric contour that represents the true geometric limb profile of Phobos. In the first method, intensity profiles across the small black reseau spots on the vidicon faceplate were used to estimate the point-spread function of the system. The second method related the integrated brightness of Phobos as seen from the earth (*4*) to the total light that Phobos removes from the martian surface in frame 7F91, both of which are dependent on the average reflectivity and mean radius of the satellite. A solution arises from the fact that these two parameters are characterized by distinctly different functional relations between the mean radius and the average reflectivity (Fig. 2). However, a phase correction must be made because the difference in phase angle between the terrestrial telescopic observations (approximately 0°) and 7F91 (22°) cannot be ignored. Gehrels (*5*) has suggested that the phase coefficient probably falls within the range 0.025 to 0.030 magnitude/degree, and I accepted the average as a nominal value.

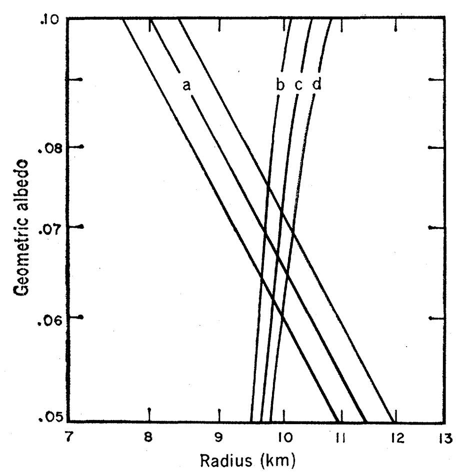


Fig. 2. Relation between the radius and average geometric albedo of Phobos for (i) a mean opposition magnitude of + 11.6 (*a*) with ± 0.1 magnitude uncertainty limits; and (ii) obstruction of light from the martian surface, corrected for phase coefficients of 0.04 (*b*), 0.03 (*c*) and 0.02 (*d*). The intersection of (*a*) and (*c*) gives a mean radius of 10 km and an average geometric albedo of 0.065.

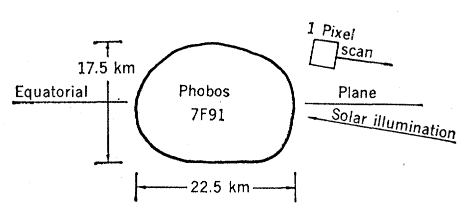


Fig. 3. Limb profile of Phobos in frame 7F91. The size of a single television picture element (pixel) and vidicon scanning direction is indicated. The orbital plane of Phobos (not shown) lies nearly in the martian equatorial plane. Geometric corrections and coherent noise removal have changed the shape from that seen in the raw version (Fig. 1).

These two methods gave consistent results. The point-spread function estimated from the reseau intensity profiles led to a Phobos limb profile measuring 18 by 22 km. With Gehrels' estimate for the phase coefficient, the second method gave a mean radius of 10 km, somewhat larger than earlier estimates (*6*), and average reflectivities of 0.065 and 0.038 at phase angles of 0° and 22°, respectively. I refer to the zero-phase reflectivity hereafter as the geometric albedo. Figure 3 shows the limb profile of Phobos in frame 7F91 as suggested by the above analysis.

Before proceeding further it would be appropriate to define the sources of error. Figure 2 shows the effects of the estimated 10-percent uncertainty in the integrated brightness (*4*) and the 0.02 to 0.04 limits of the assumed phase coefficient (*5*) of Phobos. These uncertainties have very little effect on the mean radius, and even the geometric albedo is confined to range between 0.059 and 0.074. In reporting these results I am still unable to include those errors introduced by certain poorly understood nonlinear properties of the Mariner vidicons. However, estimates of the magnitude of these errors suggest that the effects will be small in comparison to those described above.

The most significant result of this study is the very low geometric albedo (0.065) of Phobos. This value is lower than that known for any planet, satellite, or asteroid in the solar system. Previously, the smallest known value was 0.100, the geometric albedo of Mercury; the geometric albedos of the moon and Mars average 0.115 and 0.154, respectively (*7*).

Just why Phobos should have so dark a surface is not immediately obvious, Darkening of surface silicates by solar proton bombardment as observed on the moon does not explain the still lower reflectivity of Phobos, because Phobos receives less than 50 percent of the solar particle flux received by the moon. Perhaps the low albedo of Phobos can be explained by its relatively dust-free surface. Like all small satellites and asteroids, Phobos has a correspondingly small escape velocity of 12 m/sec (8). However, unlike small asteroids which can encounter meteoritic dust approaching with negligible relative velocity, Phobos must suffer impacts from particles moving with relative velocities of not less than 0.9 km/sec, nearly 100 times greater than the escape velocity. This general relation between impact and escape velocities will occur for any very small satellite moving deep within the gravitational field of its massive primary. We might then imagine Phobos, and perhaps Deimos as well, as having a surface continuously sputtered clean by meteoritic particles.

Phobos is elongated in the plane of its orbit (Fig. 3). The elongation along the line of sight is of course unknown, but we can infer from Fig. 3 that the ratio of maximum to minimum diameter is at least 1.3, a significant departure from spherical symmetry. This result should not be surprising for a small rigid body, which is unable to adjust its physical surface to a gravitational equipotential surface. It does suggest, however, that Phobos did not form by accretion as it orbited within the planetesimal cloud around primordial Mars, but may have been captured in its present form at some later time. That Phobos may have had its origin within the asteroid belt is not an unreasonable supposition.

Finally, the true anomaly of Phobos was advanced approximately 2 to 3° with respect to its ephemeris position. Uncorrected geometrical distortion in the far-encounter photographs limits the accuracy to which we can measure the areocentric position of Phobos at present. In a later paper we expect to be able to report improved orbital elements of Phobos.

BRADFORD A. SMITH
*The Observatory, New Mexico State University, Las Cruces 88001*

**References and Notes**

1. R. B. Leighton, N. H. Horowitz, B. C. Murray, R. P. Sharp, A. H. Herriman, A. T. Young, B. A. Smith, M. E. Davies, C. B. Leovy, *Science* **166**, 49 (1969).
2. A time separation of only 85 seconds between frames 6F40 and 6F41 provides near-redundancy to optimize detection of the satellite and its shadow.
3. Phobos was 130,900 km from the spacecraft when frame 7F91 was taken. This corresponds to an image scale of 3.5 km per pixel.
4. Observations by G. P. Kuiper give a mean opposition visual magnitude of $11.6 \pm 0.1$ for Phobos as reported by D. L. Harris [in *Planets and Satellites*, G. P. Kuiper and B. M. Middlehurst, Eds. (Univ. of Chicago Press, Chicago, 1961), p. 289].
5. Based on observed phase coefficients of small asteroids (T. Gehrels, personal communication) I have taken values of 0.02 and 0.04 magnitude/degree as extremes of the phase coefficient of Phobos.
6. By using Kuiper's mean opposition visual magnitude of $+11.6$ and adopting the martian geometric albedo of 0.154, one arrives at a mean radius of 6.5 km for Phobos. This value is typical of many earlier estimates of the size of Phobos.
7. Geometric albedos are taken from D. L. Harris [in *Planets and Satellites*, G. P. Kuiper and B. M. Middlehurst, Eds. (Univ. of Chicago Press, Chicago, 1961), p. 307]. They are all "visual" albedos, corresponding to the $V$ spectral band of the UBV system, and are measured at an effective wavelength of 550 to 560 nm. The effective wavelength of the Mariner television camera which took frame 7F91 is approximately 560 nm; therefore the geometric albedo of Phobos may be regarded as the visual value, $p(V)$.
8. This value is based on a mean density of 2.8 g/cm$^3$, the average for the earth's crust. The escape velocity varies with the square root of the mean density.
9. I thank T. B. Kirby for measurements of the orbital position of Phobos, S. A. Dean for assistance with the hand correction of the photometric data, and B. C. Murray and R. B. Leighton for suggestions. I also thank the project personnel at the Jet Propulsion Laboratory, particularly G. E. Danielson, S. A. Collins, and J. A. Dunne for assistance.

30 March 1970

## Paleomagnetism and Gondwanaland

Abstract. *Lower Paleozoic data now available for all the southern continents enable a unique reconstruction of Gondwanaland to be determined from paleomagnetic measurements alone. This reconstruction is corroborated by the computerized fit of the continental shelves and the matching of geological age provinces.*

We have recently completed some paleomagnetic measurements on lower Paleozoic formations from India (*1*) and Australia (*2*). For the first time, lower Paleozoic paleomagnetic data are available for each of the southern continents. These data, together with the upper Paleozoic results, now make it possible to reconstruct Gondwanaland uniquely from paleomagnetic results alone. The purpose of this report is to present such a reconstruction and to show that it is supported by the geological evidence previously used to favor an alternative Gondwanic configuration.

Early paleomagnetic studies of various Mesozoic rock formations from the southern continents (*3, 4*) demonstrated the occurrence of relative movement between these land masses since Mesozoic times (*4*). The African and Austrialian results (*4*) showed that during the Mesozoic era the pole remained stationary with respect to both continents, so that, in effect, only one average Mesozoic pole position was determined for each. A single pole places a continent in latitude and azimuthal orientation, but the longitude remains indeterminate. Thus the configuration of the southern land masses prior to continental drift could not be determined uniquely from the Mesozoic data. However, the relative positions of two or more continents can be determined without ambiguity from paleomagnetic data if they have remained in a fixed position relative to each other during a period in which substantial polar wandering occurred (*5*). Results from Africa (*6*) and South America (*7*) indicate that this condition was satisfied during most of the Paleozoic era, for it has been shown that the polar-wander paths for the two continents are almost coincident for most of the Paleozoic if the South Atlantic is closed (*8*).

Briden has noted that Paleozoic paleomagnetic poles from the Gondwanic continents tend to group about three stable positions that occur in the intervals Cambrian to Lower Devonian, Devonian to Lower Carboniferous, and Upper Carboniferous to Permian, respectively (*9*). These "quasi-static intervals" were separated by short periods of time in the Devonian and Carboniferous, during which the pole moved from one stable position to the next. We may therefore reconstruct the relative locations of the Gondwanic continents during the Paleozoic if the respective paleomagnetic poles corresponding to at least two of these stable positions are determined. Our new results for the lower Paleozoic of India and Australia complete these requirements for four of the five Gondwanic continents. However, the single lower Paleozoic pole for Antarctica (*10*) is sufficient to define its position because of constraints imposed by the adjoining continents.

In Table 1 the paleomagnetic poles that have been determined for the Paleozoic of each of the southern continents have been summarized. In each case the result has been derived through the use of cleaning techniques, so that we can be reasonably sure that secondary components of magnetization have been removed and that the primary component is represented by the result.